Islamic Azad University

Journal of

Optoelectronical Nanostructures

Winter 2025; Vol. 10, No. 3: 58-70

Research Paper (Pape Type)

Precise Prognosis of Hypercholesterolemia and Acute Kidney Diseases by Photonic Crystal Biosensor

Atefeh Chahkoutahi
Department of Electrical Engineering, Delvar branch, Islamic Azad University, Boushehr, Iran

Received: 2025.04.08
Revised: 2025.09.14
Accepted: 2025.09.23
Published: 2025.11.30

Use your device to scan and read the article online

Keywords:
Kidney diseases, Biosensor, Cholesterol, Creatinine, Photonic crystal

Abstract

In this research, a 2-D photonic crystal based hexagonal shaped system is presented. The designed device is consisted of 35*42 silicon rods (placed in air). Main functionality processes of the proposed biosensor were studied by considering photonic bandgap (PBG) and field distribution spectra. PBG and field diagrams could be obtained by using plane wave expansion (PWE) and finite-difference-time-domain (FDTD) numerical techniques. The designed system could be used for prognosis of cholesterol and creatinine levels in blood (these biological elements are introduced through their refractive indices). At defined wavelengths, incident signal could be transferred along the system and would reach outputs 1 or 2. Output1 could be applied for prognosis of cholesterol concentrations with quality factor (Q): (55.2 – 66.4), sensitivity (S): 1204.7nm/RIU, detection limit (DL): (0.0021–0.0031) RIU and figure of merit (FOM): (48.18–54.6) RIU^{-1}. Output2 would be used for detection of creatinine with (Q): (175.7–195.5), (S): 1957.3nm/RIU, (DL): (4.8e-4 –5.2e-4) RIU and (FOM): (184.8–205.9) RIU^{-1}. Based on the results, proposed device (biosensor) would aid physicians in diagnosis of various serious diseases.

Citation: Atefeh Chahkoutahi. Precise Prognosis of Hypercholesterolemia and Acute Kidney Diseases by Photonic Crystal Biosensor. **Journal of Optoelectronical Nanostructures. 2025; 10(3): 58-70.**

***Corresponding author:** Atefeh Chahkoutahi
Address: Department of Electrical Engineering, Delvar branch, Islamic Azad University, Boushehr, Iran
Email: atchahkoutahi@iau.ac.ir
DOI: https://doi.org/10.71577/jopn.2025.1203483

1. INTRODUCTION

Nowadays, many scientists concentrated their works on light wave-based systems. This is due to their (optical structures) very low cost and size, high capacity and speed and easy integration. As known, optical configurations operate based on characteristics of photons. This is the main reason of their high functionalities compared with electronic based configurations (that operate based on characteristics of electrons) [1-3]. As a result, optical based systems have been increasingly designed and fabricated. In the designation process of optical system, all of the circuit parts must be optically designed (should operate based on optical principles). Therefore, system elements like waveguides, filters [4], gates [5-7], sensors [8], multiplexers and etc. must operate based on optical principles [9-11]. Optical based system can be considered based on different configurations such as plasmon [12], graphene [13], photonic crystal (PhC) and etc. PhC systems attracted enormous attentions due to their simpler configuration, extreme efficiency and ignorable cost. PhC devices can be designed in 1, 2 or 3 dimensions with circular, hexagonal or cubic periodicities. PhC devices can be designed in a periodic format in a defined substrate (dielectric like air). Distance between rods (periodicity) can be defined by lattice constant [14]. Refractive index (RI) is another parameter defining specifications of the materials considered for rods and background (Si used for rods and air for background). Photonic bandgap (PBG) is another important parameter for defining PhC based system. It can demonstrate allowed (guided) and non-allowed (forbidden) transmission wavelengths. PBG would be achieved through using PWE technique.

As known, in permitted regions, light wave would be transmitted in the system. In these wavelengths, very low amounts of the signal can reach output port and most the signal would be dispersed. While, in non-permitted regions light cannot be transmitted in the system. Light wave will oscillate between rods. This reflection (oscillation) process can help signal to be transmitted along the system. Total internal reflection (TIR) is the phenomena defining light transmission in the structure in non-permitted wavelengths [15-19]. light wave propagation in the system would be obtained by considering FDTD technique. As known, in optical integrated circuits (OICs), all devices would be defined based on optical configurations (like PhCs). Optical biosensors as important OIC's devices would also be d based defined by optical configurations. These systems would be used for diagnosis of numerous bio-marks [20-22]. Regular detection of various bio-marks such as cholesterol, hemoglobin, glucose, and creatinine are so crucial. Among the mentioned blood factors, detecting hemoglobin and glucose amounts would aid doctors in diagnosis of anemia and

diabetes [23]. Extra amounts of cholesterol and creatinine can lead to hypercholesterolemia and acute kidney diseases [24]. Therefore, detecting cholesterol and creatinine would help doctors in prognosis of mentioned illnesses.

In a research [25], a cholesterol detection sensor was suggested by using a 1-D hyperbolic PhC. Very considerable amounts were calculated for S, DL and FOM. In another research [26], by using PCFs, cholesterol amounts were detected. In [27], by proposing a sensor made of GO/PPy/PANI/ZnO combinations, cholesterol could be diagnosed. Considerable S, DL and FOM were extracted. In [24], by considering 1-D PhC system based on MgF_2 and CeO_2, an efficient sensor for diagnosis of creatinine amounts was designed. Acceptable S factor of 306.25 nm/RIU was obtained. In [28], a device based on various combinations was proposed for detection of creatinine amounts. Designed sensor indicated S factor of 1562.5nm/RIU. In the presented work, functional and remarkable PhC sensor structure would be proposed for prognosis of vital bio-marks. PBG and field diagrams are obtained for two different output ports (each port is considered for detection of cholesterol or creatinine). In the last section, the designed system is used as a biosensing element for prognosis of cholesterol and creatinine at output ports 1 and 2, respectively.

2. PRINCIPLE AND DESIGNATION

The device is made of 35*42 Si cells. Maxwell's equations are used for evaluating the system:

$$\frac{\partial B}{\partial t} = -\nabla * E - J \tag{1}$$

$$\frac{\partial B}{\partial t} = \nabla * H - J \tag{2}$$

In the above equations, D, B and J stand for displacement, magnetic induction field and current density. E and H declare electric magnetic fields.
Q-factor is an important sensing parameter [29, 30].

$$Q = \frac{\lambda_0}{\Delta\lambda_{FWHM}} \tag{3}$$

Sensitivity is another important factor.

$$S = \frac{\Delta\lambda}{\Delta n}(nm/RIU) \tag{4}$$

DL is another vital factor defined in Eq. (5).

$$DL = \frac{\lambda}{10SQ}\,(RIU) \tag{5}$$

FOM is another vital factor.

$$FOM = \frac{SQ}{\lambda}\,(RIU^{-1}) \tag{6}$$

Proposed device is depicted in Fig. 1.

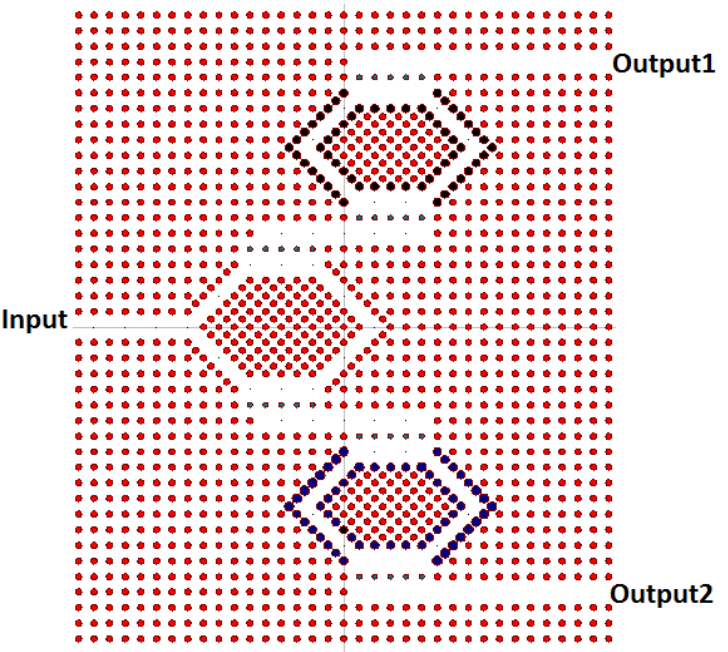

Fig. 1. Presented 2-D PhC device

As seen in Fig. 1, proposed device is made of 35*42 cells in air medium. In the presented device, linear cells were used to ease the design and fabricating techniques. In proposed device, numerous defects are designed in order to function properly (filtering specific wavelength at each output port).

As shown in the above schematic, dark blue and black cell's radius were not the same as other rod's radius. Mentioned rods function as the confinement

medium for sensing functionalities. They are able of filtering resonant wavelengths.

Dark cyan cells can be considered as coupling ones. Various structural constants of the above figure are summarized in the following table.

Table. 1. Geometrical Factors of Fig. 1

Parameter	Value
Red rod's radius	0.1μm
Dark blue rod's radius	0.13μm
Black rod's radius	0.13μm
Dark cyan rod's radius	0.09μm
Lattice constant (a)	0.5μm
Refractive index of rods	3.5

After designing the presented system (Fig. 1), PBG would be obtained. This diagram helps in investigating allowed and non-allowed wavelengths. PBG spectrum is indicated in Fig.2.

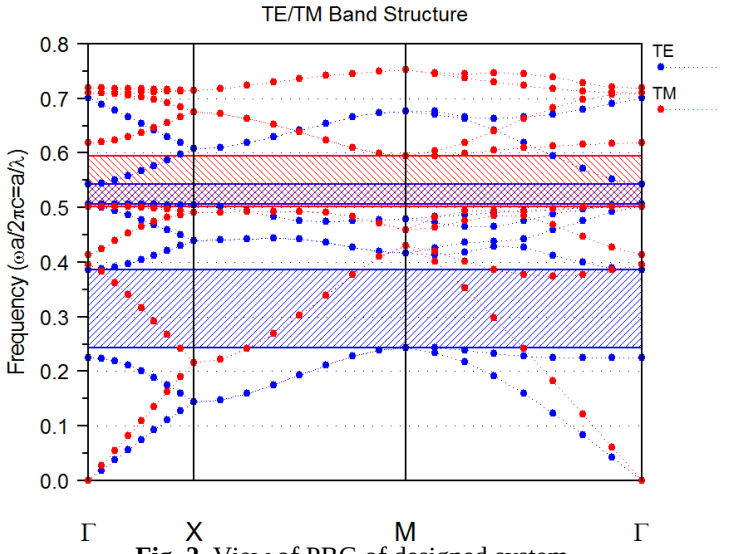

Fig. 2. View of PBG of designed system

According to Fig. 2, different modes could be achieved for designed structure. TE modes were placed 1.25μm<λ<2.08μm and 0.909μm<λ<1μm. TM modes are also placed in 0.83μm<λ<1μm. According to Fig. 2, TE PBGs were placed in wider wavelength regions. At wavelengths placed in TE region field would move through the system based on TIR effect. In next sections, distribution of electric filed at λ=1050nm, λ=1400nm and λ=1700nm would be considered.

Then, transmission-wavelength diagrams for different concentrations of cholesterol and creatinine would be extracted (from which important parameters like S, Q-factor, FOM and DL would be obtained).

3. SIMULATIONS AND RESULTS

In the presented section, field and transmission-wavelength figures are achieved by using incident field at different wavelengths.

3.1. (λ=1050nm)

In this part, electric signal at λ=1050nm (which is not involved TE PBG region) is achieved. As indicated in Fig. 3, signal is dispersed in system. Therefore, basically very low amounts of field would be transferred to outputs.

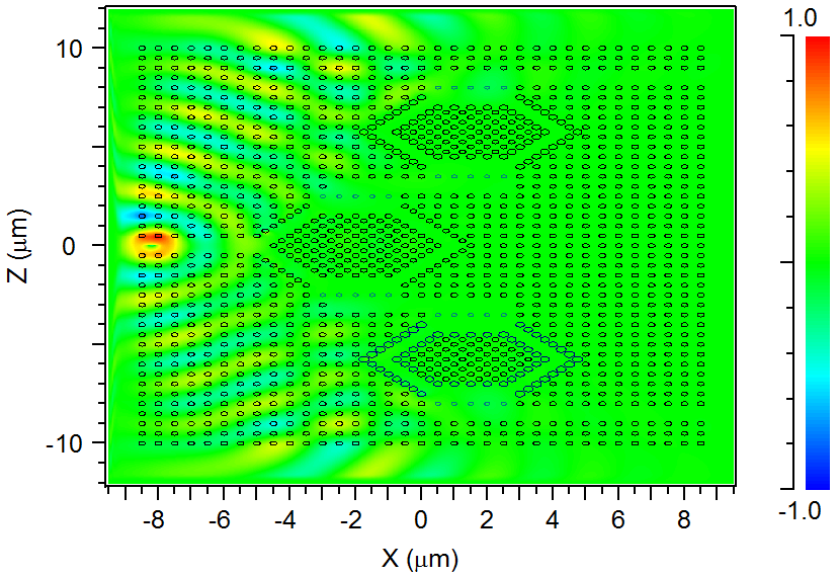

Fig. 3. View of the field at λ=1050nm

As shown in Fig. 3, very low sections of incident signal reached Outputs 1 or 2 (λ=1050nm was placed in TE guided ranges; thus, incident field would be totally faded). As a result, λ=1050nm wouldn't be useful and functional for sensing applications.

3.2. Output1 (λ=1400nm)

In this section, electric field and transmission diagrams at λ=1400nm are considered. Field distribution figure is indicated in Fig. 4. a.

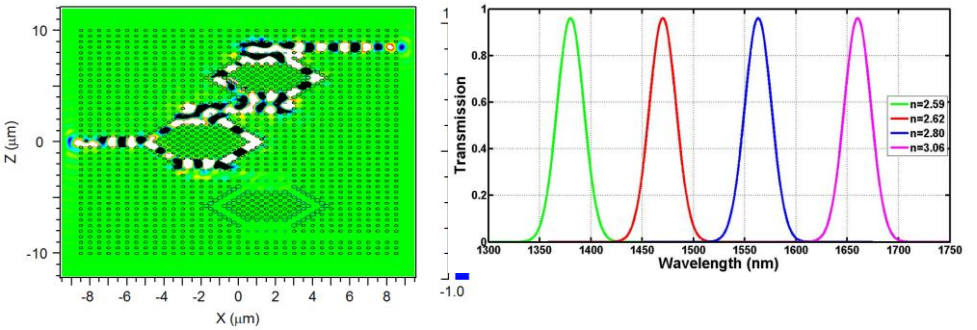

(a) (b)

Fig. 4. a) View of the electric field at λ=1400nm, b) Transmission diagram vs. wavelength for various concentrations of cholesterol in blood

As shown in Fig. 4. a, much of the input filed is transferred to output1 (λ=1400nm is placed in TE PBG ranges). Therefore, it is a functional wavelength for sensing applications. At this point, different amounts of cholesterol in blood are considered as the analyte (each cholesterol concertation is defied by its RI) and transmission-wavelength spectrum would be obtained. As previously stated, high levels of cholesterol can cause hypercholesterolemia, which can be effectively and precisely diagnosed (by this structure). Changes of resonance wavelength with respect to different amounts of cholesterol in are shown in Fig. 4. b (as transmission vs. wavelength diagram)

As known, acceptable cholesterol concertation should be lower than 200mg/dl (5.17mmol/L). As a result, cholesterol amounts more than 200mg/dl might cause danger and may lead to heart diseases [25, 31]. RIs of various Cholesterol amounts would be stated in the following table [25].

Table 2. RIs of Cholesterol Levels

Levels (mg/dl)	RIs
200	2.59
220	2.62
240	2.80
260	3.06

As seen in Fig. 4. b, increasing RI enhances central wavelength of the diagram (wavelength is moved to extreme values) [32, 33]. S, Q-factor, FOM and DL can be obtained as follows (for output1) through Fig. 4. b, and Eqs. (3-6):
Q: (55.2–66.4), S: 1204.7nm/RIU, DL: (0.0021–0.0031) RIU, FOM: (48.18–54.6) RIU^{-1}. All in all, the proposed biosensor would remarkably aid researchers in prognosis of hypercholesterolemia.

3.3 Output2 (λ=1700nm)

In this part, electric filed and transmission diagrams at λ=1700nm are considered. Field spectrum is shown in Fig. 5. a.

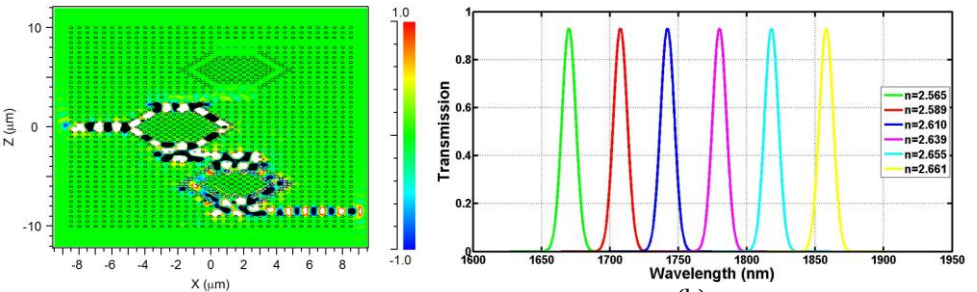

(a) (b)

Fig. 5. a) View of the field at λ=1700nm, Transmission-wavelength diagram for different amounts of creatinine

As can be shown in Fig. 5. a, most of input signal (at λ=1700nm) was transferred to output2. This phenomenon happened due to the fact that λ=1700nm is situated in TE PBG range. Thus, it will be a good wavelength for sensing functionalities. In the next step, various creatinine concentrations in blood will be investigated. According to the obtained result, transmission-wavelength spectrum will be achieved. Considering the obtained results, acute kidney diseases might be precisely and prognosed by physicians. Alterations in the resonance wavelength through applying various values of creatinine in blood can be seen in Fig. 5. b.

RIs defined in Fig. 5. b are summarized in following table 3 [24].

Table 3. RIS of Creatinine Levels

Levels (µmol/L)	RIs
85.28	2.565
84.07	2.589
83.3	2.610
82.3	2.639
81.43	2.655
80.9	2.661

According to Fig. 5. b, enhancing refractive index can lead to the movement of peak wavelength to higher values [32, 33]. Through Fig. 5. b and EqS. (3-6), important bio sensing parameters related to output2 would be achieved as following. Q: (175.7–195.5), S: 1957.3nm/RIU, DL: (4.8e-4 –5.2e-4) RIU, FOM: (184.8–205.9) RIU^{-1}. All in all, researchers can precisely prognosis acute kidney injuries. Obtained results of the proposed sensor (for outputs 1and 2) are compared with previously reported researches and are mentioned in Table. 4.

Table 4. Comparison of Proposed Sensors with Previous Ones

References	Sensitivity (nm/RIU)	FOM (RIU^{-1})	Q-factor	LOD (RIU)
Cholesterol [25]	469	125		0.0091
Cholesterol [34]	156.18	10.41		
Cholesterol [35]	245.6714	13.5	28	
Proposed Cholesterol	**1204.7**	**48.18–54.6**	**55.2 – 66.4**	**0.0021–0.0031**
Creatinine [28]	1562.5			
Creatinine [24]	306.25			
Creatinine [36]	637	10.3		
Proposed Creatinine	**1957.3**	**184.8–205.9**	**175.7–195.5**	**4.8e-4 –5.2e-4**

4. CONCLUSON

A functional PhC biosensor made of 35*42 silicon in air was presented. Different important diagrams were obtained through PWE and FDTD techniques. Various defect rods were introduced for conducting the interfering and scattering phenomenon. The designed device was presented for prognosis of cholesterol and creatinine at specific wavelengths (situated in the TE PBG region). Characteristics of the biosensor at output1 (detection of cholesterol) were, Q: (55.2 – 66.4), S: 1204.7nm/RIU, DL: (0.0021–0.0031) RIU and FOM: (48.18–54.6) RIU^{-1}. Considering these parameters, physicians can diagnose

hypercholesterolemia in early stages. The proposed biosensor at output2 was considered for detection of creatinine with Q: (175.7–195.5), S: 1957.3nm/RIU, DL: (4.8e-4 –5.2e-4) RIU and FOM: (184.8–205.9) RIU^{-1}. Finally, presented system could be an appropriate choice for bio-sensing applications in optical integrated circuits.

REFERENCES

[1] F. Parandin, A. Sheykhian, Design and simulation of a 2 × 1 All-Optical multiplexer based on photonic crystals, Optics & Laser Technology. 151 (2022) 108021. Available: https://doi.org/10.1016/j.optlastec.2022.108021

[2] E. Rafiee, F. Emami, Design of a Novel All-Optical Ring Shaped Demultiplexer based on Two-Dimensional Photonic Crystals, Optik. 140 (2017) 873-877. Available: https://doi.org/10.1016/j.ijleo.2017.05.010

[3] F. Parandin, High contrast ratio all-optical 4 × 2 encoder based on two-dimensional photonic crystals, Opt. Laser Technol. 113 (2019) 447–452. Available: https://doi.org/10.1016/j.optlastec.2019.01.003

[4] E. Rafiee, F. Emami, Design and Analysis of a Novel Hexagonal Shaped Channel Drop Filter Based on Two-Dimensional Photonic Crystals, JOPN. 1 (2) (2016) 39-46. Available: https://journals.marvdasht.iau.ir/article_2047.html.

[5] F. Pakrai, et al., Designing of All-Optical Subtractor via PC-Based Resonators, JOPN. 7 (2) (2022) 21--36. Available: 10.30495/jopn.2022.29545.1246.

[6]] B. Elyasi, S. Javahernia, All optical digital multiplexer using nonlinear photonic crystal ring resonators, JOPN. 7 (1) (2022) 97- 106. Available: 10.30495/jopn.2022.29174.1242.

[7] F. khatib, M. Shahi, Ultra-Fast All-Optical Symmetry 4×2 Encoder Based on Interface Effect in 2D Photonic Crystal, JOPN. 5 (3) (2020) 103- 114. Available: 20.1001.1.24237361.2020.5.3.7.6.

[8] M. Momeni, et al., Design of High Sensitivity and high FoM Refractive Index Biosensor Based on 2D-Photonic Crystal, JOPN. 6 (1) (2021) 33- 58. Available: 10.30495/jopn.2022.27033.1217.

[9]] E. Rafiee, et al., Design of a Novel Nano Plasmonic-Dielectric Photonic Crystal Power Splitter Suitable for Photonic Integrated Circuits, Optik. 172 (2018) 234-240. Available: https://doi.org/10.1016/j.ijleo.2018.06.006

[10]] F. Parandin, R. Kamarian, M. Jomour, A novel design of all optical half-subtractor using a square lattice photonic crystals, Opt Quant Electron. 53 (2021) 114. Available: https://doi.org/10.1007/s11082-021-02772-8

[11]] F. Parandin, et al., Design of 2D photonic crystal biosensor to detect blood Components, Opt Quant Electron. 54 (2022) 618. Available: 10.21203/rs.3.rs-1459722/v1
[12] V. Zayets, at al., Fabrication technique for low-loss plasmonic waveguides incorporating both "plasmonic-friendly" and "plasmonic-unfriendly" metals, Photonics Nanostructures. 57 (2023) 101196. Available: https://doi.org/10.1016/j.photonics.2023.101196
[13] A. Ahmadianyazdi, et al., Glucose measurement via Raman spectroscopy of graphene: Principles and operation, Nano Res. 15, 8697–8704 (2022). Available: https://doi.org/10.1007/s12274-022-4587-9
[14] G. Palai, et al., Optical MUX/DEMUX using 3D photonic crystal structure: A future application of silicon photonics, Optik 128 (2017) 224–227. Available: https://doi.org/10.1016/j.ijleo.2016.10.019
[15] A. Vahdati, F. Parandin, Antenna patch design using a photonic crystal substrate at a frequency of 1.6 THz, Wireless Pers. Commun. 109 (2019) 2213–2219. Available: https://doi.org/10.1007/s11277-019-06676-5
[16] F. Parandin, M. Moayed, Designing and simulation of 3-input majority gate based on two-dimensional photonic crystals, Optik 216 (2020) 164930. Available: https://doi.org/ 10.1016/j.ijleo.2020.164930
[17] F. Parandin, Ultra-compact terahertz all-optical logic comparator on GaAs photonic crystal platform, Opt. Laser Technol. 144 (2021) 107399. Available: https://doi.org/ 10.1016/j.optlastec.2021.107399
[18]] F. Parandin, F. Heidari, Z. Rahimi, S. Olyaee, Two-dimensional photonic crystal Biosensors: A review, Opt. Laser Technol. 144 (2021) 107397. Available: https://doi.org/ 10.1016/j.optlastec.2021.107397
[19] A. Askarian, Design and analysis of all optical 2 × 4 decoder based on kerr effect and beams interference procedure, Opt Quant Electron 53 (2021) 291. Available: https://doi.org/10.1007/s11082-021-02987-9
[20] E. Rafiee, et al., Hypercholesterolemia diagnosis by a biosensor based on photonic crystal PANDA structure, Opt Rev. 31(2024) 87–93. Available: https://doi.org/10.1007/s10043-023-00859-z
[21] F. Parandin, et al., A comprehensive review of blood component detection utilizing One-Dimensional, Two-Dimensional, and photonic crystal fiber biosensors, Results Opt. 16 (2024) 100671. Available: https://doi.org/10.1016/j.rio.2024.100671
[22] N. Tasnim, et al., Highly sensitive photonic crystal fiber based surface plasmon resonance biosensor for detection of wide range of organic solutions, Sens. Bio-Sens. Res. 43 (2024) 100623. Available: https://doi.org/10.1016/j.sbsr.2024.100623

[23] A. Panda, et al., Performance analysis of graphene-based surface plasmon resonance biosensor for blood glucose and gas detection, Appl. Phys. A. 126 (2020). Available: DOI:10.1007/s00339-020-3328-8

[24] A. H. Aly, D. Mohamed, M. A. Mohaseb, N. S. Abd El-Gawaad, Y. Trabelsi, Biophotonic sensor for the detection of creatinine concentration in blood serum based on 1D photonic crystal, RSC Adv. 10 (2020) 31765. Available: https://doi.org/10.1039/D0RA05448H.

[25] D. Dash and J. Saini, Hyperbolic Graded Index Biophotonic Cholesterol Sensor with Improved Sensitivity, Prog. Electromagn. Res.M. 116 (2023) 165-176. Available: doi:10.2528/PIERM23032302

[26]] M. Rahman, et al., Photonic crystal fiber based terahertz sensor for cholesterol detection in human blood and liquid foodstuffs, Sens. Bio-Sens. Res. 29 (2020) 100356. Available: https://doi.org/10.1016/j.sbsr.2020.100356

[27] A. Kumar, et al., Ultrahigh sensitive graphene oxide/conducting polymer composite based biosensor for cholesterol and bilirubin detection, Biosens. Bioelectron: X. 13 (2023) 100290. Available: https://doi.org/10.1016/j.biosx.2022.100290

[28] R. Negahdari, et al., Sensitive MIM plasmonic biosensors for detection of hemoglobin, creatinine and cholesterol concentrations, Diam. Relat. Mater.136 (2023) 110029. Available: https://doi.org/10.1016/j.diamond.2023.110029

[29] Y. F. Gao, et al., Design of novel power splitters by directional coupling between photonic crystal waveguides, Optoelectron. Lett. 6 (2010) 417–420. Available: https://doi.org/10.1007/s11801-010-0017-4.

[30] S. Olyaee, et al., Two-curve-shaped biosensor using photonic crystal nano-ring resonators, JNS. 4 (2014) 303–308. Available: https://jns.kashanu.ac.ir/article_7996.html

[31] H. Ma, Cholesterol and Human Health, Nat. Sci. 2 (4), (2004) 17-21. Available: https://www.jofamericanscience.org/journals/am-sci/0201/05-mahongbao-0105.pdf

[32] H. T. Chorsi, et al., Tunable plasmonic substrates with ultrahigh Q-factor resonances, Sci. Rep. 7 (2017) 15985. Available: https://doi.org/10.1038/s41598-017-16288-3

[33] A. Chahkoutahi, et al., Sensitive Hemoglobin Concentration Sensor Based on Graphene‐Plasmonic Nano‐structures, Plasmonics. 17 (2022) 423–431. Available: DOI: 10.1007/s11468-021-01531-5

[34] Y. Lu, H. Li, X. Qian, W. Zheng, Y. Sun, B. Shi and Y. Zhang, Beta-cyclodextrin based reflective fiber-optic SPR sensor for highly-sensitive

detection of cholesterol concentration, Opt. Fiber Technol. 56 (2020) 102187. Available: https://doi.org/10.1016/j.yofte.2020.102187.

[35] X. Fu, D. Li, Y. Zhang, G. Fu, W. Jin and W. Bei, High sensitivity refractive index sensor based on cascaded core-offset splicing NCF-HCF-NCF structure, Opt. Fiber Technol. 68, (2022) 102791. Available: https://doi.org/10.1016/j.yofte.2021.102791

[36] S. Gandhi, S. K. Awasthi and A. H. Aly, Biophotonic sensor design using a 1D defective annular photonic crystal for the detection of creatinine concentration in blood serum, RSC Adv. 11 (2021) 26655-26665. Available: https://pubs.rsc.org/en/content/articlelanding/2021/ra/d1ra04166e